EFFECT OF TRANSITION METALS ON THE TENSILE PROPERTIES OF 354 ALLOY: ROLE OF PRECIPITATION HARDENING

G. H. Garza-Elizondo, A. M. Samuel, and F. H. Samuel
Université du Québec à Chicoutimi, Chicoutimi, QC, Canada

S. Valtierra
Nemak, S.A., P.O. Box 100, 66221 Garza García, N.L., Mexico

Abstract

The present study was carried out to investigate the effects of minor additions of Ni and Zr, individually or in combination, on the microstructure and tensile properties of 354 casting alloy (Al–9 wt%Si–1.8 wt%Cu–0.5 wt%Mg) at room temperature (25 °C/77 °F) and at high temperatures (155 and 300 °C/311 and 572 °F) using different holding times at testing temperature. An analysis of the data obtained from microstructural and tensile tests shows that the tensile behavior of 354-type cast alloys is strongly influenced by the testing temperature and the holding time at temperature prior to testing. The effect of minor additions of Ni and Zr on the high-temperature performance of these alloys is controlled by their T6-properties at room temperature. The addition of 0.2 wt% Ni and 0.2 wt% Zr improves the T6-tensile properties considerably, compared to the as-cast condition. The addition of 0.4 wt%
Ni + 0.4 wt% Zr is not sufficient to resist softening at 300 °C (572 °F)/100 h. The addition of 0.4 wt% Ni to alloy 354 leads to a decrease in the tensile properties, attributed to a Ni–Cu reaction that interferes with the formation of Al_2Cu strengthening precipitates and affects the age-hardening process. The fine $L1_2$ ($Al_3(Zr,Ti)$)-type precipitates is the main feature observed in the microstructure of alloys containing 0.2–0.4 wt% Zr additions. The presence of Q-$Al_5Cu_2Mg_8Si_6$ phase and Al_3Ni phase is observed in samples tested at 300 °C (572 °F) after 10 h holding.

Keywords: aluminum alloys, additives, high-temperature testing, precipitation hardening, phase identification, nickel, zirconium

Introduction

The addition of alloying elements is often used to improve the structure, mechanical properties and hence quality of aluminum casting alloys. Traces of Sr are added to Al alloys containing Si to modify the Si particle morphology from coarse flakes to a finer fibrous form. Other studies show that the absorption of Sr by Fe-intermetallics refines their morphology considerably.[1–3] Titanium and boron are added either individually or in combination to refine the grain structure of α-Al by providing large numbers of nuclei in the melt, inducing the formation of small equiaxed grains of α-Al rather than a coarse, columnar grain structure. Zirconium is used as a grain refiner and can also be used to form fine coherent Al_3Zr dispersoids which are stable at high aging temperatures and resist coarsening due to the low solubility and diffusivity of Zr in the Al matrix. Nickel is added to Al–Cu and Al–Si alloys to improve both hardness and strength parameters at elevated temperatures as well as to reduce the coefficient of thermal expansion.[4]

Aluminum casting alloys containing Cu and Mg are 'heat-treatable alloys' whose strength is improved via precipitation hardening using suitable heat treatment regimes. Aging, the final stage of the heat treatment process, is an important treatment and involves strengthening the alloys by coherent precipitates which are capable of being sheared by dislocations.[2] This stage consists of maintaining the alloy at a certain temperature for a sufficient period of time to permit the solute atoms to precipitate in the form of finely dispersed metastable phases. By controlling the aging time and temperature, a wide variety of mechanical properties may be obtained; tensile strength can be

increased, residual stresses can be reduced, and the microstructure can be stabilized.

The precipitation process can occur at room temperature (natural aging) or may be accelerated by artificial aging at a temperature ranging from 90 to 260 °C (194 to 500 °F). The idea of aging is to obtain a uniform distribution of small precipitates, which gives high strength to the alloy.[3,4] When a longer aging time may be needed, it becomes necessary to promote precipitation by using higher temperatures or artificial aging.[5]

Aging of an aluminum alloy containing copper as the alloying element results in the formation of various forms of Al–Cu-containing precipitates. The precipitation sequence of an Al–Cu alloy during the aging process has been proposed as follows:[6–8]

$$\alpha(SSS) \rightarrow \text{GP zones} \rightarrow \theta'' \rightarrow \theta' \rightarrow \theta$$

The coherent and semi-coherent phases, θ'' and θ', respectively, contribute to increasing the alloy strength. On the other hand, the incoherent equilibrium precipitate θ (Al_2Cu) results in diminishing the hardening level of the alloys because of the loss of coherency between the stable phases and the metal matrix. For an aluminum alloy containing Cu and Mg as the hardening elements, the aging treatment results in the formation of a range of precipitates.

The generally accepted sequence of precipitation in Al–Cu–Mg alloys is: θ-Al_2Cu precipitate and its precursors, along with other hardening phases/precipitates such as the S-Al_2CuMg phase and its precursors, which are observed to form during the aging treatment of an aluminum alloy containing Cu and Mg.[9,10] The formation of the S phase during aging treatment occurs via the following precipitation sequence:[6,11–15]

$$\alpha(SSS) \rightarrow \text{GP zones} \rightarrow S'' \rightarrow S' \rightarrow S$$

starting with the decomposition of the supersaturated solid solution (SSS), followed by the formation of GPB zones, and then by the precipitation of the coherent S'', the semi-coherent S', and finally the incoherent S (Al_2CuMg) equilibrium phase. The S'' and S' precipitates are responsible for increasing the strength level of such alloys, whereas overaging results in the precipitation of the incoherent equilibrium S phase. There is another phase containing Si which may form in the Al–Cu–Mg–Si system, called the Q phase or quaternary $Al_5Cu_2Mg_8Si_6$ phase which may form upon solidification or during aging.[16–19]

The Q phase can also coexist with Al_2Cu, Mg_2Si, and Si depending on the ratio between Cu, Mg, and Si. One of the suggested mechanisms for the formation of the Q phase is that the Cu atoms dissolve in the β'' phase which then evolves either to β (Mg_2Si) or to the Q phase, based on the chemical composition of the alloy and precipitation status.[20,21]

Alloys such as A354 and C355 (containing Al, Si, Cu, and Mg) are increasingly used in automotive applications where thermal stability is an important requirement particularly in critical parts. The presence of more stable Cu-based inter-metallic compounds in the A354 alloy is expected to ensure superior thermal stability as compared to the more widely used A356/A357 alloys.[22] The present study was therefore undertaken to examine the room and high-temperature performance of 354 (Al–9 wt%Si–1.8 wt%Cu–0.5 wt%Mg) casting alloys containing different alloying elements, in order to determine their effect on the tensile properties of automotive castings under actual operating conditions. In light of this objective, an analysis of the precipitates formed as a result of the various alloying and heat treatment conditions used was carried out, where a field emission scanning electron microscope (FESEM) equipped with energy-dispersive X-ray spectrometric (EDS) and wavelength dispersion spectrometric (WDS) systems was used to examine the characteristics (i.e., size, distribution and density) of the hardening precipitates in the 354 alloys investigated, for the various aging temperatures and times involved.

Experimental Procedures

The 354 casting alloy used in this study was supplied in the form of 12.5-kg ingots. The chemical composition of the 354 base alloy (coded G1) is presented in Table 1. The alloy ingots were melted in a 40-kg capacity SiC crucible, using an electrical resistance furnace. The melting temperature was maintained at 750 ± 5 °C to ensure complete dissolution of Zr.[23] It should be mentioned here that the humidity in the surrounding media was about 23 %. All the 354 alloy melts prepared were grain-refined by adding 0.15 wt% Ti in the form of rods of Al–5 wt%Ti–1 wt%B; they were then Sr-modified using Al–10 wt%Sr master alloy, to obtain levels of 0.25 wt% Ti and ~140 ppm Sr in the melt to minimize the possibility of Sr oxidation during the melting process as well as porosity formation in the final casting. Minor additions of Ni and Zr were carried out using Al–20 wt%Ni and Al–20 wt%Zr master alloys, respectively. The master alloys were added to the base alloy melts, only instants before degassing to ensure homogeneous mixing of the additives together with the degassing. The melts were degassed for ~15–20 min with a rotary graphite impeller rotating at ~130 rpm, using pure dry argon injected into the molten metal at a constant rate of 20.4 m³/h. Following this, the melt was carefully skimmed to remove oxide layers from the surface. Figure 1 displays the RPT test performed on G1 molten alloy before and after degassing revealing the disappearance of most of the porosity in the solidified alloy (cup sample castings are shown in the figure).[24]

The melt was poured into an ASTM B-108 permanent mold preheated at 450 °C (842 °F) to drive out moisture, for preparing the tensile test bars. Samplings for chemical analysis were also taken simultaneously at the time of the

Table 1. Chemical Composition of the 354 Alloys Used in this Study

Alloy/element	Si	Fe	Cu	Mg	Ti	Sr	Ni	Zr	Al
G1[a]	9.43	0.08	1.85	0.49	0.22	0.0150	~	0.15	Bal.
G2	9.16	0.08	1.84	0.49	0.22	0.0149	0.46	0.15	Bal.
G3	9.10	0.07	1.83	0.49	0.21	0.0145	~	0.39	Bal.
G4	9.01	0.08	1.85	0.45	0.21	0.0127	0.21	0.19	Bal.
G5	9.10	0.08	1.86	0.46	0.22	0.0122	0.40	0.39	Bal.

[a] G1: 354 base alloy
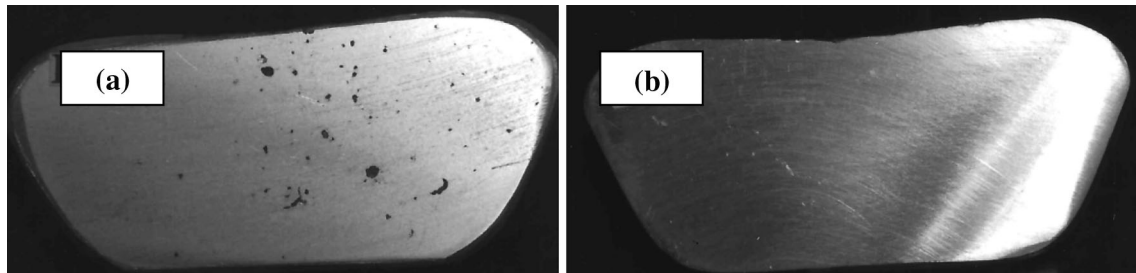
Figure 1. RPT test: (a) before degassing, (b) after degassing.

Figure 2. FESEM setup used in the present study.

casting to ascertain the exact chemical composition of each alloy. The chemical analysis was carried out using a Spectrolab-JrCCD Spark Analyzer. Table 1 lists the actual chemical compositions of the alloys produced.

Prior to heat treatment, the tensile bars were divided in bundles of five bars each. The five bars were attached tightly together using iron wire to facilitate their removal from the furnace for quenching in warm water. Tensile test bars of alloys G1, G2, G3, G4, and G5 were T6-heat treated

which comprised solution heat treating at 505 °C (941 °F) for 8 h, followed by quenching in warm water at 60 °C (140 °F). The time lapse between sample removal and quenching was about 30–40 s. The quenched bars were then artificially aged at 190 °C (374 °F) for aging times of 2, 10, 40, and 100 h. The aged samples were then pulled to fracture at 25 °C (77 °F).

The condition selected for the high-temperature tensile testing was the T6-treated (190 °C [374 °F]/2 h aged)

condition, using two selected testing temperatures (155 and 300 °C/311 and 572 °F) and holding times of 10, 40, and 100 h at each testing temperature. Tensile testing was carried out at a strain rate of $4 \times 10^{-4}\ \text{s}^{-1}$, using an Instron Universal Mechanical Testing machine. The testing was carried out at 25 °C/77 °F (for samples in the as-cast and T6-treated conditions), and at high temperature (155 and 300 °C /311 and 572 °F) using holding (or stabilization) times of 10, 40, and 100 h at testing temperature). A data acquisition system attached to the machine provided
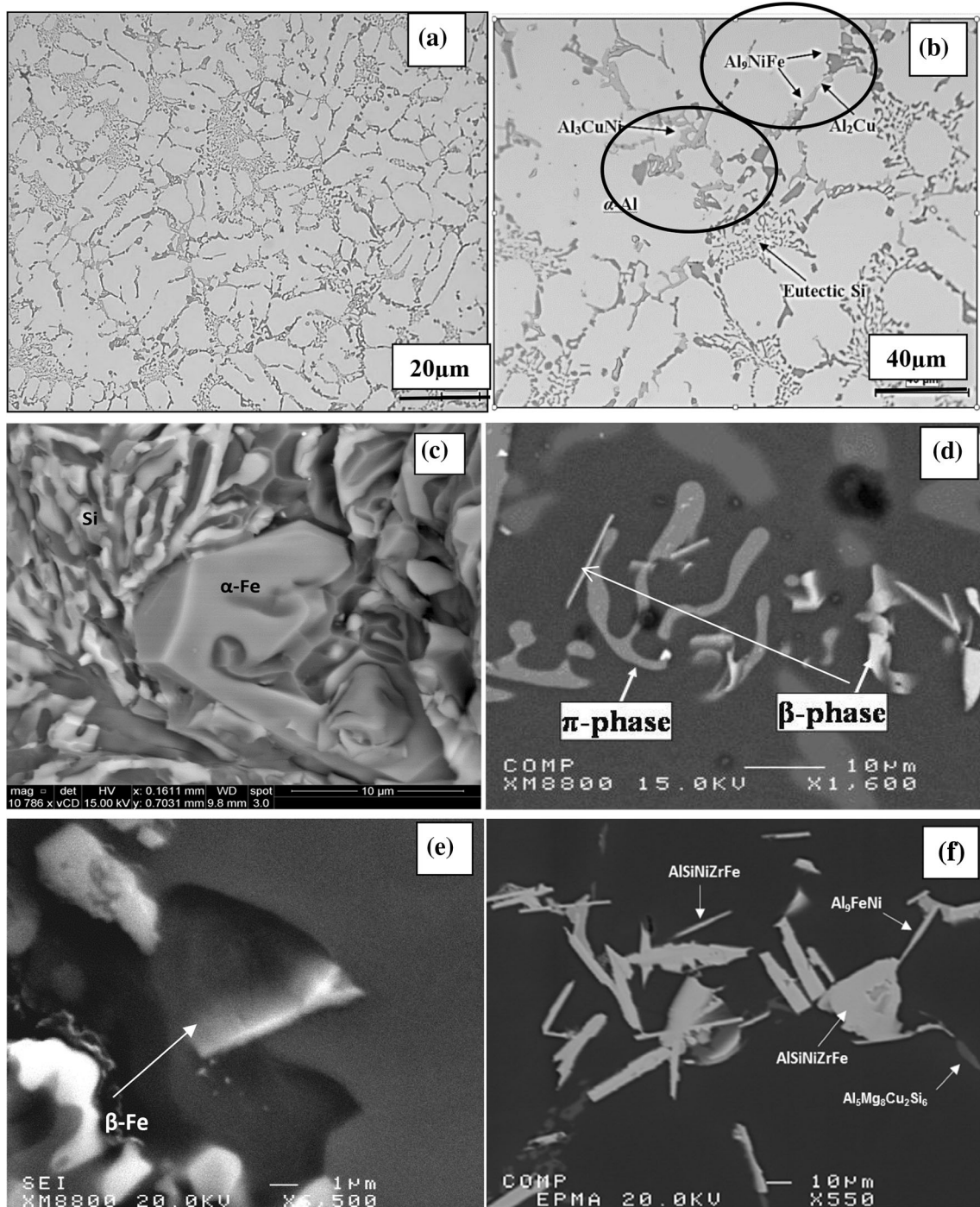
Figure 3. *Micrographs of tensile-tested samples showing (a, b) as-cast microstructure of (a) G1 alloy, and (b) G5 alloy, (c) deeply etched sample revealing the co-existence of α-Fe in the interdendritic region with the Si particles, (d) decomposition of π-Fe phase to thin β-Fe platelets in G1 alloy following solution heat treatment,[26] (e) high-magnification backscattered electron image showing the size and morphology of the newly formed β-Fe platelets. (f) Precipitation of Zr- and Ni-rich compounds in G5 alloy.*

the tensile data, namely the ultimate tensile strength (UTS), the yield strength at 0.2 % offset strain (YS), and the elongation to fracture (%El), calculated over the 25.4 mm gauge length of the tensile test bars. A total of 275 bars were tested.

Samples for metallographic examination were sectioned from the tensile-tested bars of selected alloy/conditions studied, about 10 mm below the fracture surface and polished using standard techniques. The field emission scanning electron microscope (FESEM) provides clear and less electrostatically distorted high-resolution images even at low voltages; it can produce images of 2.1 nm resolution at 1 kV and of 1.5 nm resolution at 15 kV. The instrument used in this study was a Hitachi-SU-8000 (FESEM), equipped with EDS and WDS equipment. Prior to examination, the polished sample surfaces were re-polished using ion bombardments for 20 min to minimize surface oxidation. It should be noted here that all EDS spectra were taken at 10–15 kV regardless of the accelerating voltage used for the electron micrographs. Figure 2 shows the setup used in the present work.

Results and Discussion

The temperature selected for the solution heat treatment might appear to be over-conservative but it was deemed necessary to avoid any risk of incipient melting of the copper phases, which could have the potential for deteriorating the mechanical properties of the alloys to a great extent. An increase in strength after the treatment is normally observed in similar 354 alloys which use a solution heat treatment temperature of 525 °C (977 °F), over a
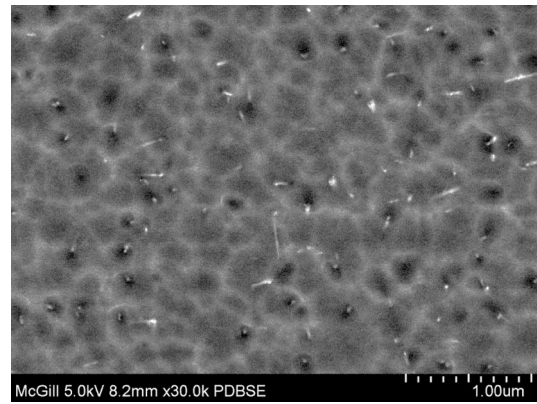

Figure 5. *Precipitation of ultra-fine particles in as-quenched G1 alloy.*

2–3 h period, in conjunction with analogous aging treatments.[25] The main objective of applying aging treatment to casting alloys containing magnesium and silicon is to precipitate the excess Mg and Si out of the supersaturated solid solution in the form of Mg_2Si hardening phase. Dislocations are known to be potential sites for Mg_2Si precipitates which would lead to a pronounced improvement in mechanical performance following artificial aging.[25]

In this study, the alloys used were modified employing about 140 ppm strontium. Therefore, it is expected that the microstructure even in the as-cast condition should have refined eutectic silicon particles with fine primary aluminum grains, the solidification rate of the casting process being relatively high. A complete modification of the silicon particles in the microstructure of alloy G1 and G5 in the as-cast condition may be observed in Figure 3a, b. In regard to alloy G5, the only observable
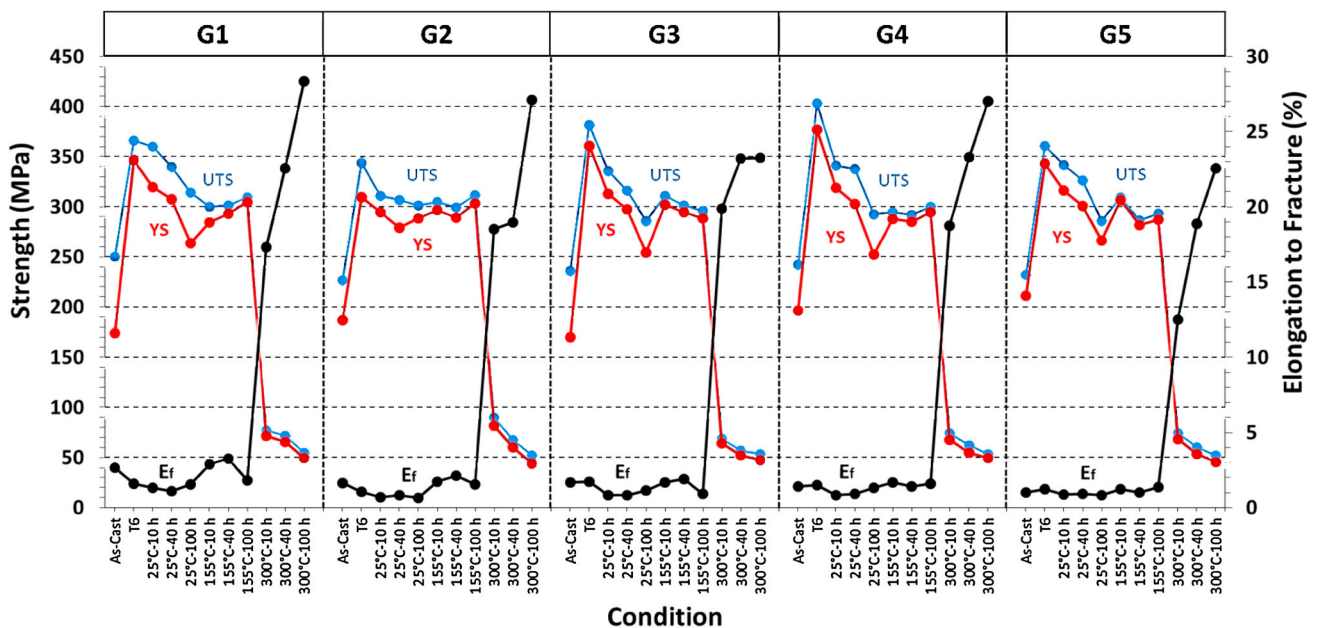

Figure 4. *Average values of ultimate tensile strength (UTS), yield strength (YS), and percentage elongation (%El) for alloys G1 to G5 tested under different conditions at room and at high temperature.*
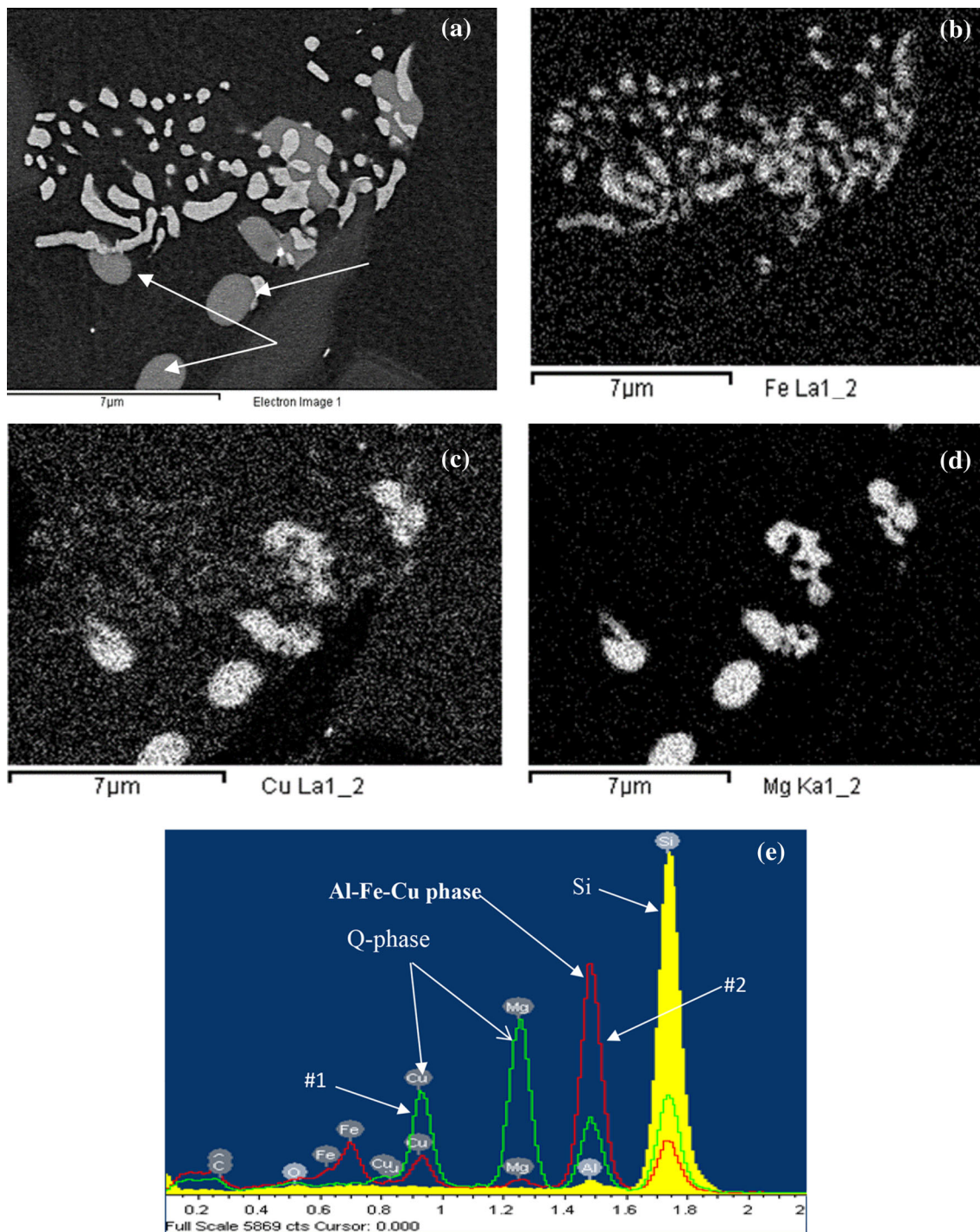
Figure 6. *(a) Backscattered electron image showing the co-existence of Q-Al$_5$Mg$_8$Si$_6$Cu$_2$ phase and Fe-based intermetallics in the as-quenched G1 alloy, (b–d) images showing distribution of Fe, Cu, and Mg elements in (a), (e) EDS spectra corresponding to the Q (#1), Al–Fe–Cu intermetallic (#2) and Si phases seen in (a).*

difference with respect to alloy G1 is the presence of Ni-based intermetallics as shown in Figure 3b-black circled areas.

Figure 4 displays the tensile properties of the five alloys investigated in this study, where it will be observed that the as-cast alloy samples exhibit tensile strength values of 225–250 MPa, giving a difference of about 10–25 MPa between the base alloy G1 (UTS 250.03 MPa) and the remaining alloys G2 (226.34 MPa), G3 (236.16 MPa), G4 (241.87 MPa), and G5 (232.07 MPa). The solution heat treatment temperature of 505 °C (941 °F) in combination with the aging temperature/time (190 °C [374 °F]/2 h) increases the alloy strength (UTS and YS) while

maintaining more or less the same ductility as that observed in the as-cast case.

After T6 treatment (aging at 190 °C [374 °F]/2 h), the strength values increase significantly, reaching peak strength in each case. The yield strength follows the same trend, exhibiting somewhat lower values compared to UTS. Alloy G4 (containing 0.2 wt% Ni + 0.2 wt% Zr) shows the maximum increase in tensile properties with a UTS of 402.93 MPa, followed by a UTS value of 381.87 MPa for alloy G3 (containing 0.4 wt% Zr) which may be attributed in part due to precipitation of $Al_3(Zr,Ti)$ phase particles.

Alloy G5 (containing 0.4 wt% Ni + 0.4 wt% Zr) displays a UTS value slightly lower than that of the base alloy G1 (360.71 vs. 365.97 MPa). On the other hand, alloy G2 (containing 0.4 wt% Ni) displays strength values that are lower than those exhibited by the base alloy in the as-cast, T6 and other aging conditions listed in Figure 4. These observations may be explained in terms of high affinity of Ni to react with Cu forming Al_6Cu_3Ni and $Al_3(Ni,Cu)_2$ intermetallics. As a result, the amount of free Cu is reduced and hence the observed decrease in the alloy strength.[1]

Increase in aging time from 10 to 100 h during T6 heat treatment continually lowers the alloy strength; the ductility is also lowered to a slight extent indicating the commencement of T7 stage. Apparently, aging time is a crucial factor that has a significant effect on the alloy strength, in particular the yield strength, causing it to reduce by as much as ~ 100 MPa, the only exception being the G2 alloy where the decrease with aging time is much slower. This trend continues at the 155 and 300 °C (311 and 572 °F) testing temperatures, until, after 100-h holding time for the tests carried out at 300 °C (572 °F), the UTS and YS values are reduced for the five alloys, with a corresponding increase in the ductility on account of alloy softening. Compared to the T6 condition (room temperature testing), the closest tensile properties obtained are those exhibited by alloy G2 at 155 °C (311 °F)/100-h holding time.

A decrease in the tensile properties of Al–Si–Cu–Mg alloys upon the addition of increasing amounts of Ni has been noted in the related literature.[27] This decrease in strength through the addition of nickel is attributed to the interaction between copper and nickel to form precipitates of Al_3CuNi in the microstructure, normally present in the alloys containing Ni, namely G2, G4, and G5 alloys. Since copper, as well as magnesium, determines the precipitation strengthening of Al–Si–Cu–Mg alloys, the formation of the Al–Cu–Ni precipitates would thus subtract part of the copper content available for strengthening through the formation of Al_2Cu precipitates. It may be possible that nickel interacts with iron and copper forming the Al_9NiFe

and Al_3CuNi phases; such phases would act as stress concentrators provoking instability in the flow strain, thereby reducing the ductility of the alloy.[1]

While Cu and Mg are added to improve the room and high-temperature strength, the development of intermetallic phases including θ-(Al_2Cu), β-(Mg_2Si), π-($Al_8Mg_3FeSi_6$), Q-$Al_5Cu_2Mg_8Si_6$,) in these alloys promotes strengthening, however, at the expense of ductility. In this context, iron impurities are the most detrimental as they lead to the
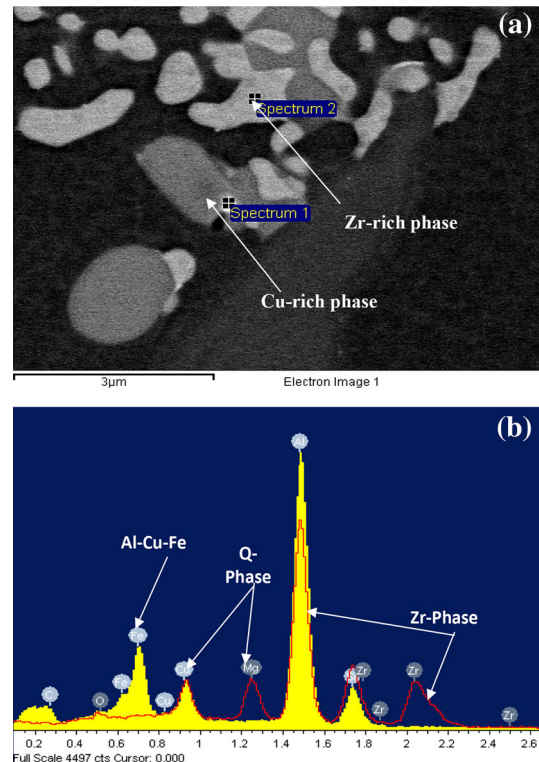

Figure 7. (a) High-magnification electron micrograph taken from G1 alloy, (b) EDS spectra revealing the presence of Zr-rich phase (red line), probably Al₃Zr, along with Al–Cu–Fe and Q phases (thin-line spectrum).
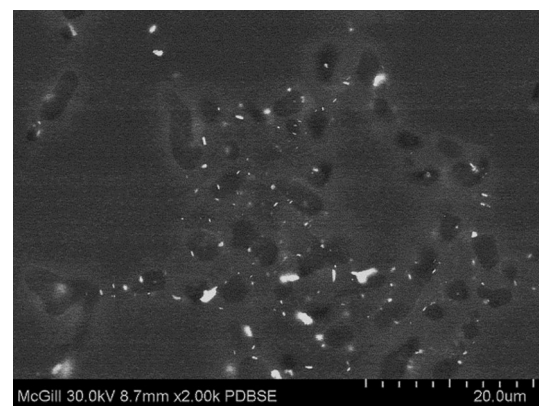

Figure 8. Precipitation observed in G1 base alloy in the T6-treated condition (190 °C/2 h aged).

development of relatively large π-(Al$_8$Mg$_3$FeSi$_6$), β-(Al$_5$FeSi) and α-(Al$_{15}$(Mn,Fe)$_3$Si$_2$) brittle intermetallics, with the π-and β-iron phases being the most harmful phases in terms of mechanical integrity.[28,29]

Taking the five alloys into consideration, and over the three holding times, the average tensile properties for the alloys may be considered to be 300 MPa UTS, 293 MPa YS, and 1.75 % elongation at 155 °C (311 °F), respectively. At the higher testing temperature of 300 °C (572 °F) and for holding times up to 100 h, the morphologies of the Zr-rich and Ni-rich intermetallic phases have a harmful influence on the mechanical properties as shown in Figure 3f.

The presence of 0.4 wt% Ni + 0.4 wt% Zr in alloy G5 is not sufficient to resist softening at 300 °C (572 °F) after 100-h holding time, so that the alloy strength decreases to 52 MPa UTS and 45 MPa YS, while the ductility increases to 23 %. At 300 °C (572 °F), for the proposed holding

times, the alloy strength begins to decrease from $\sim$75 MPa for the 10-h holding time, to reach $\sim$53 MPa after 100-h holding time for all alloys. The YS showed the same behavior as UTS. The most important results obtained at 300 °C (572 °F) after holding at 100 h are the high ductility values exhibited by all the alloys, with alloys G1 through G5 showing percent elongation values of 28.4, 27.1, 23.2, 27, and 22.6 %, respectively.

Alloy G4, containing 0.2 wt% Ni and 0.2 wt% Zr, displays greater strength than alloy G3 which contains 0.4 wt% Zr, or greater even than alloy G5 which contains 0.4 wt% Ni and 0.4 wt% Zr. The main difference, which appears upon examining the Zr content of alloys G3, G4, and G5, involves the fact that alloy G4 is a hypo-peritectic alloy.[30] According to the Al–Zr phase diagram, at 0.2 wt% Zr content, the liquidus temperature is approximately 720 °C (1328 °F). Taking into consideration the fact that the temperature of the melt was 750 °C (1382 °F) during
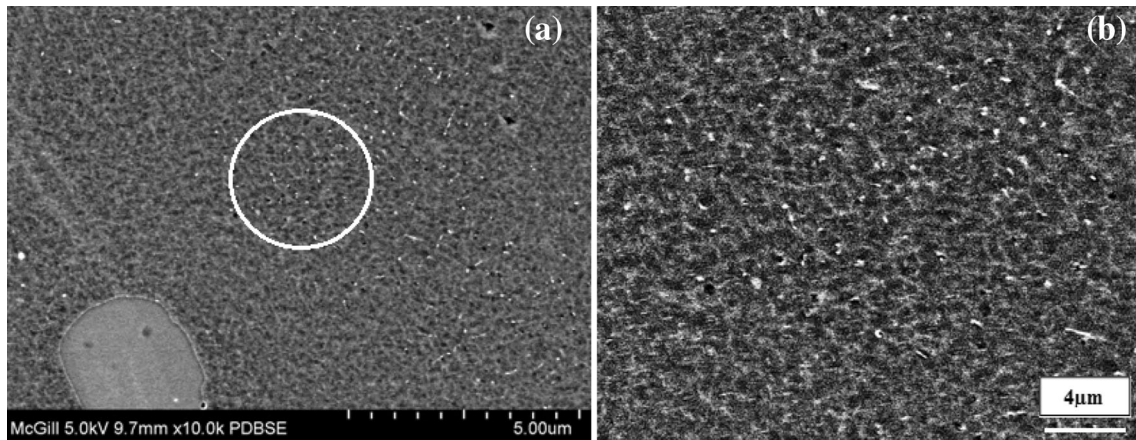

Figure 9. (a) Precipitation in T6-treated G1 alloy tested at 155 °C after holding for 10 h, (b) enlarged image of circled area in (a)-note the absence of PFZs.
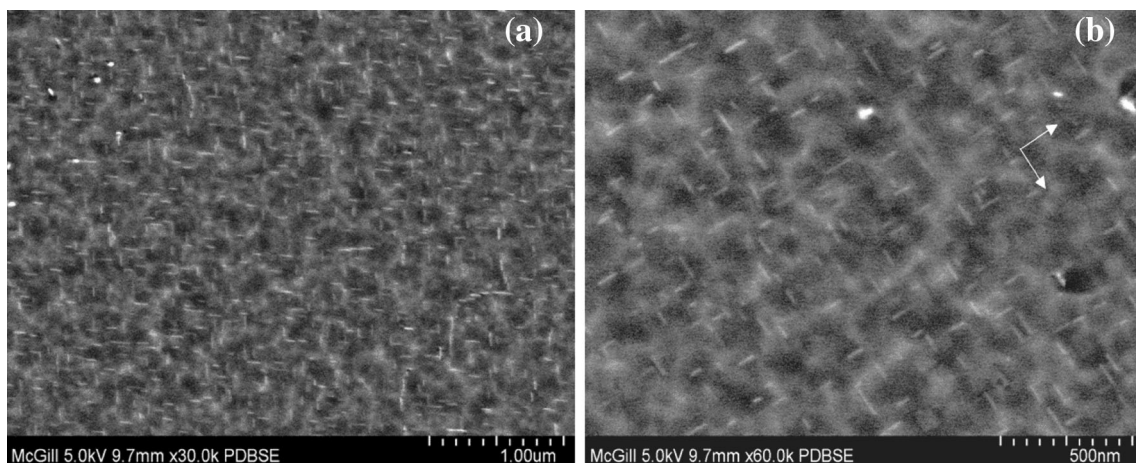

Figure 10. (a) Precipitation in T6-treated tensile sample of G1 alloy deformed at 155 °C after holding for 100 h, (b) high-magnification BSE image of (a) showing the presence of two perpendicular precipitate families—see white arrows.

casting, it is fairly likely that the added Zr dissolved completely. Having a completely dissolved Zr master alloy in the melt would be the first step in obtaining alloy strengthening by means of Zr-rich precipitates.

As was observed in the work of Knipling[31] with Al–Zr and Al–Zr–Ti alloys, Zr-rich nanoparticles precipitate during solidification forming coherent precipitates which are resistant to coarsening at temperatures in the order of 275–425 °C; such Zr-rich particles would improve the mechanical properties at 300 °C (572 °F) of the as-cast G5 alloy. It is possible that alloy G5 in T6 condition did not display the same properties as in the as-cast condition. This apparent contrast in behavior could be explained by the fact that the alloys in the T6 condition were submitted to a solution heat treatment at 505 °C (941 °F) which would change the coherency of the Zr-rich precipitates formed during the solidification of alloy G5.

In a study of the aging behavior of 319-type Al–Si–Cu–Mg alloys, Andrade[32] observed that, initially, the Al_2Cu precipitates formed are evenly distributed and uniformly sized. As a preferential precipitate grows, it draws atoms from the surrounding precipitates, which in turn reduces the total number of precipitates within the aluminum matrix. With fewer precipitates present, the average distance or spacing between neighboring precipitates increases, and thus it is easier for slip plane movement to occur. This is an important point, in view of the fact that the force required to cut through a precipitate is inversely proportional to the precipitate spacing. Once this critical size and precipitate spacing are reached, the tensile strength will begin to decrease.

Age hardening of such Al–Si–Cu–Mg alloys results in the precipitation of the Q phase and its precursors, which play an essential role in the strengthening of this specific alloy system. Similarly, in addition to the precipitation of the Q phase ($Al_5Cu_2Mg_8Si_6$), several others, such as θ-Al_2Cu, β-Mg_2Si, S-Al_2CuMg, σ-$Al_5Cu_6Mg_2$ and their precursors, are also expected to precipitate during age-hardening treatment of 354 type Al–Si–Cu–Mg alloys; the Cu-containing precipitates such as Q phase ($Al_5Cu_2Mg_8Si_6$) and θ-Al_2Cu are the strengthening particles obtained in the T6-tempered alloys.

As mentioned earlier, the objective of applying aging treatment to casting alloys containing magnesium and silicon is to precipitate the excess Mg and Si out of the supersaturated solid solution in the form of Mg_2Si
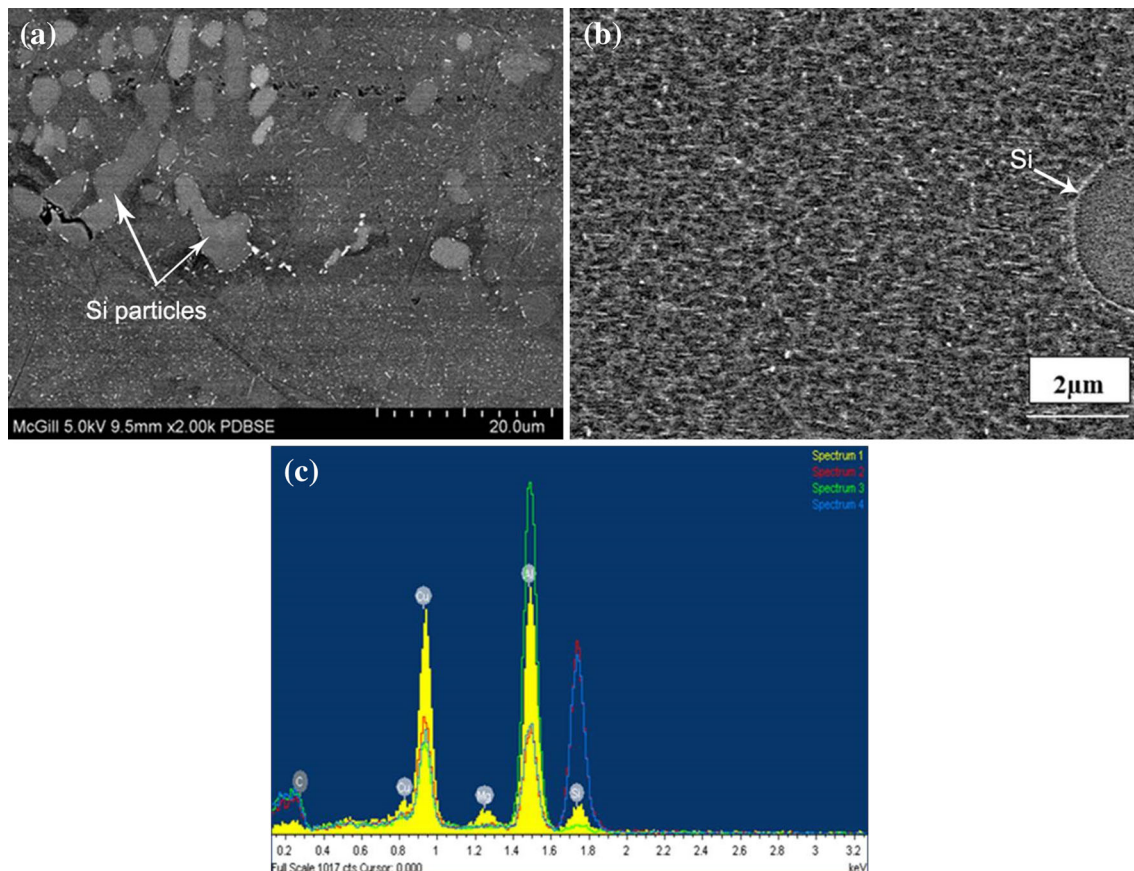

Figure 11. Backscattered electron images of T6-treated G1 alloy tensile sample held for 10 h at 300 °C prior to deformation (a) general view, (b) high-magnification image, (c) EDS spectra obtained from different particles showing strong reflections of Al and Cu elements.

hardening phase. Dislocations are known to be potential sites for Mg_2Si precipitates which would lead to a pronounced improvement in mechanical performance following artificial aging.[24,25] Figure 5 shows precipitation of θ-Al_2Cu phase particles in the as-quenched sample of the base alloy G1. (The black spots appearing in this micrograph are the result of the ion bombardment). This precipitation may have taken place during the period between quenching and phase examination (3 days).

Figure 6a shows clusters of undissolved Q phase ($Al_5Mg_8Si_6Cu_2$) phase (gray particles) in certain regions covered with spheroidized Fe-based intermetallic (grayish white) particles; the corresponding X-ray images of Fe, Cu, and Mg shown in Figure 6b–d supports these observations. Figure 6e is a compilation of three EDS spectra obtained from the Q, Al–Cu–Fe–Mg-based intermetallic, and Si phase particles seen in Figure 6a, revealing the presence of reflections due to Al, Si, Cu, Mg, and Fe. It should be borne in mind that all tensile samples subjected to high-temperature testing were used in the T6-treated condition. Figure 7 reveals the existence of the Q phase and a Zr-rich phase, mainly Al_3Zr in G1 alloy, as inferred from the associated EDS spectra (#1 and #2, respectively) shown in Figure 7b. The observed Mg and Cu peaks in

Figure 7b may be due to the fact that the Zr-rich particle is overlapping a particle of Q phase.

Aging the solutionized G1 alloy at 190 °C (374 °F) for 2 h resulted in precipitation of θ-Al_2Cu phase as displayed in Figure 8. Thereafter, holding the T6-treated tensile sample of G1 alloy at 155 °C (311 °F) testing temperature for 10 h resulted in a marked increase in the density of precipitated particles, as shown in Figure 9a. As the higher-magnification image of the encircled area shown in Figure 9b reveals, the particles are more or less spherical.

Increasing the holding time to 100 h at 155 °C (311 °F) prior to deformation resulted in changing the morphology of the precipitates into thin platelets distributed in two perpendicular directions, as displayed in Figure 10. Tavitas-Medrano et al.[33–36] carried out an intensive transmission electron microscopic investigation on the morphology of the precipitating phase in 319 alloy samples aged at 170 °C (338 °F) for 8 h. Their results showed that in the peak aging condition, or aging at 170 °C (338 °F) for 8 h, the microstructure shows a dense homogeneous precipitation of θ'-Al_2Cu plates which are the main contributor to strengthening in 319-type alloys, oriented in the <100>
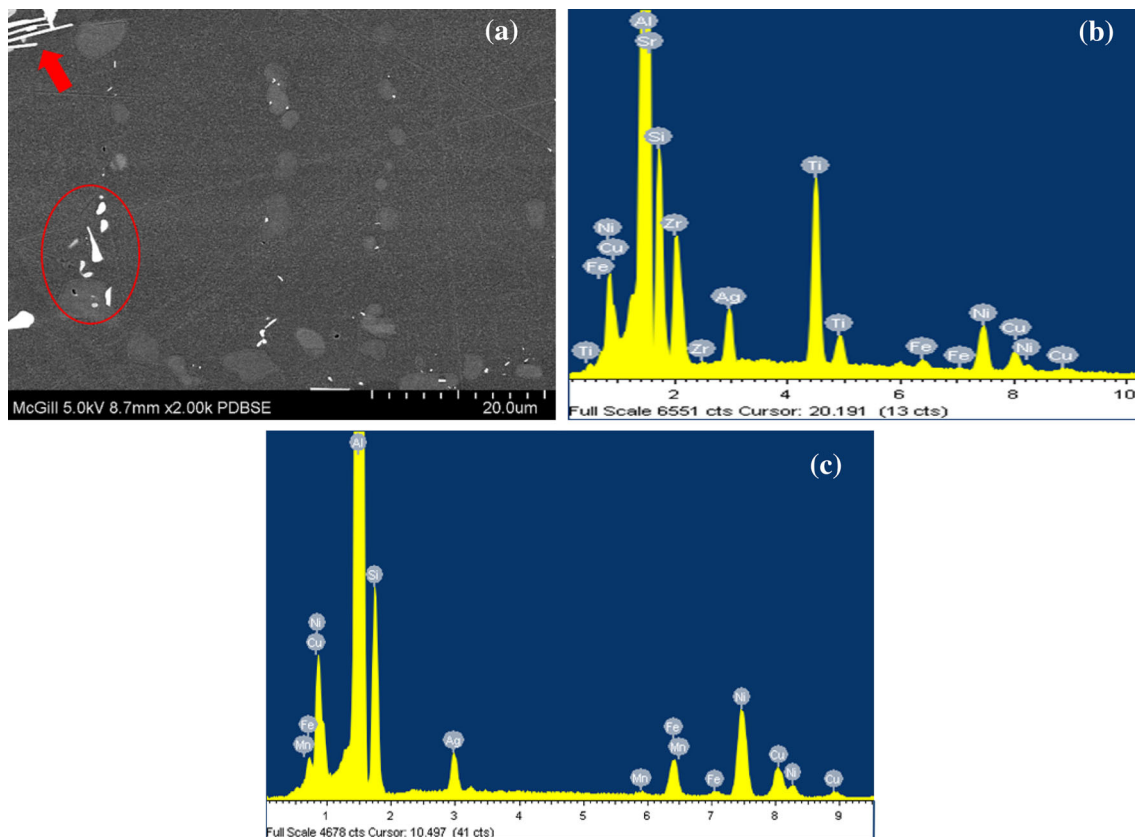

Figure 12. (a) Backscattered electron image of G5 alloy following solution treatment/quenching, (b) EDS spectrum corresponding to the circled area in (a), and (c) EDS spectrum obtained from the arrowed area in (a) showing peaks due to Al, Si, Ni, Cu, and Fe.
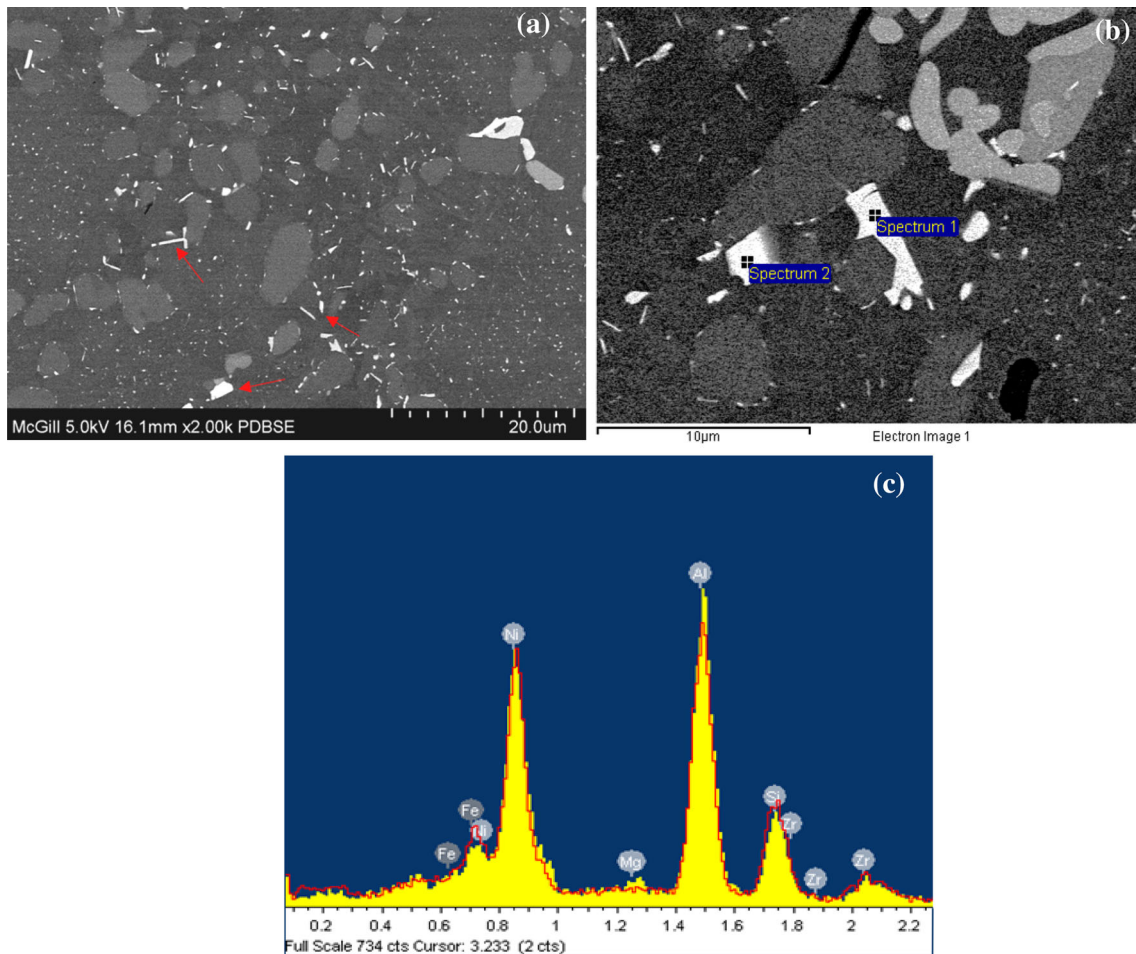
Figure 13. *(a) BSE image of T6-treated tensile sample of G5 alloy held at 300 °C/10 h prior to deformation, (b) high-magnification electron image of (a), (c) EDS spectrum obtained from the bright particles arrowed in (a) reveals that these particles are mainly Al₃Ni phase. Spectrum #1 and spectrum #2 are overlapped in (c).*
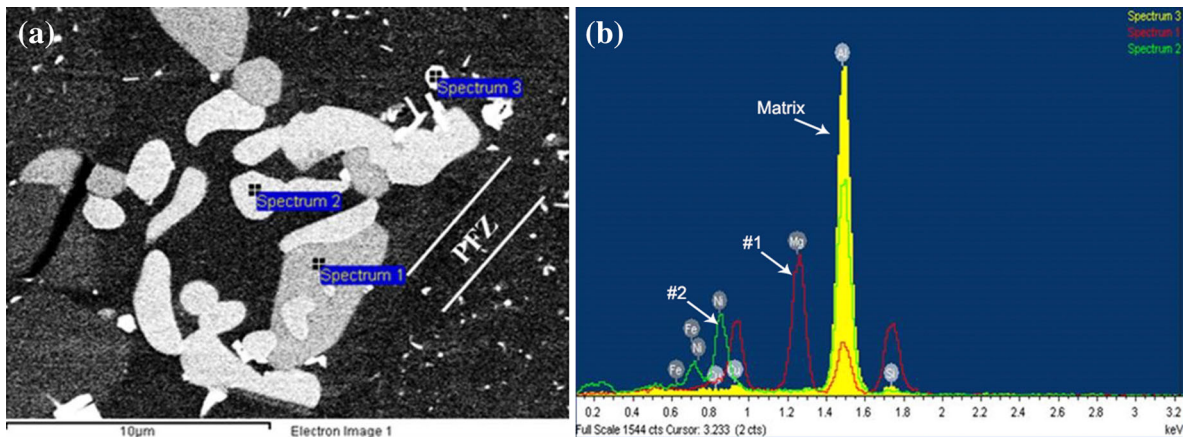

Figure 14. *(a) High-magnification image of insoluble phases observed in G5 alloy, (b) EDS spectra corresponding to different areas in (a) indicate the presence of Q-Al₅Mg₈Si₆Cu₂ phase (#1) and Al₃Ni phase (#2). Note the presence of precipitate-free zones (marked PFZ) in (a).*

directions of the matrix; these plates display an average size of 5 × 35 nm. Similar observations have been reported by Ringer and Hono.[8] As mentioned previously, precipitation of the Al₂Cu phase starts with the formation of Guinier–Preston (GP) zones which consist of copper layers in the {100} matrix planes, followed by precipitation of the semi-coherent θ' phase and finally formation of the equilibrium Al₂Cu phase.[37]
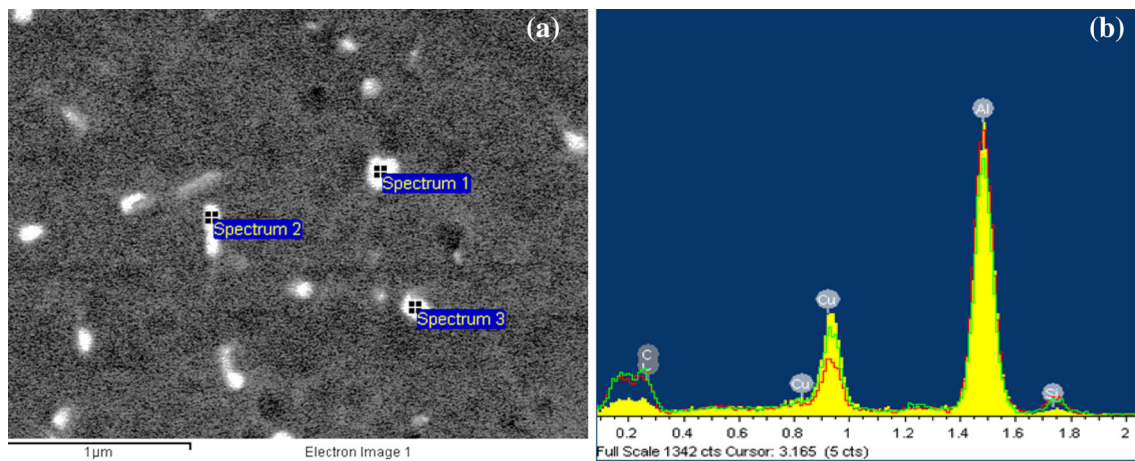
Figure 15. *(a) Backscattered electron image of the fine precipitates observed in the T6-treated tensile sample of G5 alloy shown in Figure 13a, (b) EDS spectra corresponding to different particles in (a), displaying strong peaks of Al and Cu elements.*

Figure 11 reveals that by increasing the testing temperature to 300 °C (572 °F), the density of precipitated particles markedly increased, visually reaching that obtained from samples held at 155 °C (311 °F) for 100 h. The morphology of the precipitates is more or less in the form of thin platelets, about 0.2 μm in size, Figure 11b—measurements were made at 100,000×. The associated EDS spectra obtained from different precipitates and shown in Figure 11c indicated that most of these precipitates are of Al_2Cu type.

Figure 12a presents the microstructure of G5 alloy obtained after solution heat treatment/quenching, revealing the presence of Zr-rich phase particles (circled in red). The associated EDS spectrum, Figure 12b, reveals strong reflections due to Al, Zr, Ti, and Ni elements. Zirconium, however, tends to interact with Ti forming a complex compound of $Al_x(Zr,Ti)$ Si.[38] The presence on Ni in Figure 12b may be associated with Cu, forming Cu_3NiAl_6 phase[39] which is insoluble during solution heat treatment.[40] Figure 12c is an EDS generated from the arrowed area in (a), showing the possible presence of Al_9FeNi phase.

In the aged condition, the $L1_2$ $(Al_3(Zr,Ti))$-type precipitates formed are coherent with the Al matrix, have high anti-phase boundary energy and low misfit. These precipitates have extreme thermal stability. Thus, with increasing temperature, they would coarsen at a slow rate. These small and dispersed $Al_3(Zr,Ti)$ particles will provide a large force to retard the movement of dislocations and increase the alloy strength[37] which may explain the reason for the observed higher strength of the aged modified alloys in the present work.

The BSE image of Figure 13a is a general view of the T6-treated tensile sample of G5 alloy showing the precipitation which occurred during 10-h holding time at 300 °C. Several bright particles may be observed, surrounding the preexisting ones (see arrows). The corresponding EDS

spectra (yellow and red) in Figure 13b reveal that these particles are mainly Al_3Ni phase. The details of insoluble phases in G5 alloy are shown clearly in Figure 14a. Figure 14b displays the EDS spectra obtained from different locations in Figure 14a, indicating the presence of Q-$Al_5Mg_8Si_6Cu_2$ phase and Al_3Ni phase.

Figure 15a presents a high-magnification image of the fine precipitates observed in Figure 13a. The corresponding EDS spectrum, shown in Figure 15b, displays peaks of Al and Cu elements. Figure 16 exhibits the precipitation characteristics and distribution when the T6-treated tensile samples of G5 alloy were held for 100 h at 300 °C (572 °F) before pulling to fracture. Figure 16a displays a general view, showing the size and distribution of the precipitated phase particles that formed under these holding conditions. It is interesting to note there are no precipitate-free zones (PFZ) around the preexisting phases (Figure 16b). Figure 16c, d indicate that these precipitates are mainly Al_2Cu phase. A relatively high-magnification image of Figure 16a is shown in Figure 16e and reveals the platelet morphology (approximately 0.1 μm thick and 1 μm long) of the precipitated phase particles in two perpendicular directions, similar to those observed in the case of the G1 alloy samples under the same working conditions.

Conclusions

In this article, the results pertaining to the influence of minor additions and various heat treatment parameters on the precipitation in Al–Si–Cu–Mg 354-type alloys and their effect on the tensile properties have been presented. Based on an analysis of these results, the following conclusions may be drawn.

1.   The Q phase ($Al_5Cu_2Mg_8Si_6$) and θ-Al_2Cu are the predominant precipitates found in the as-cast
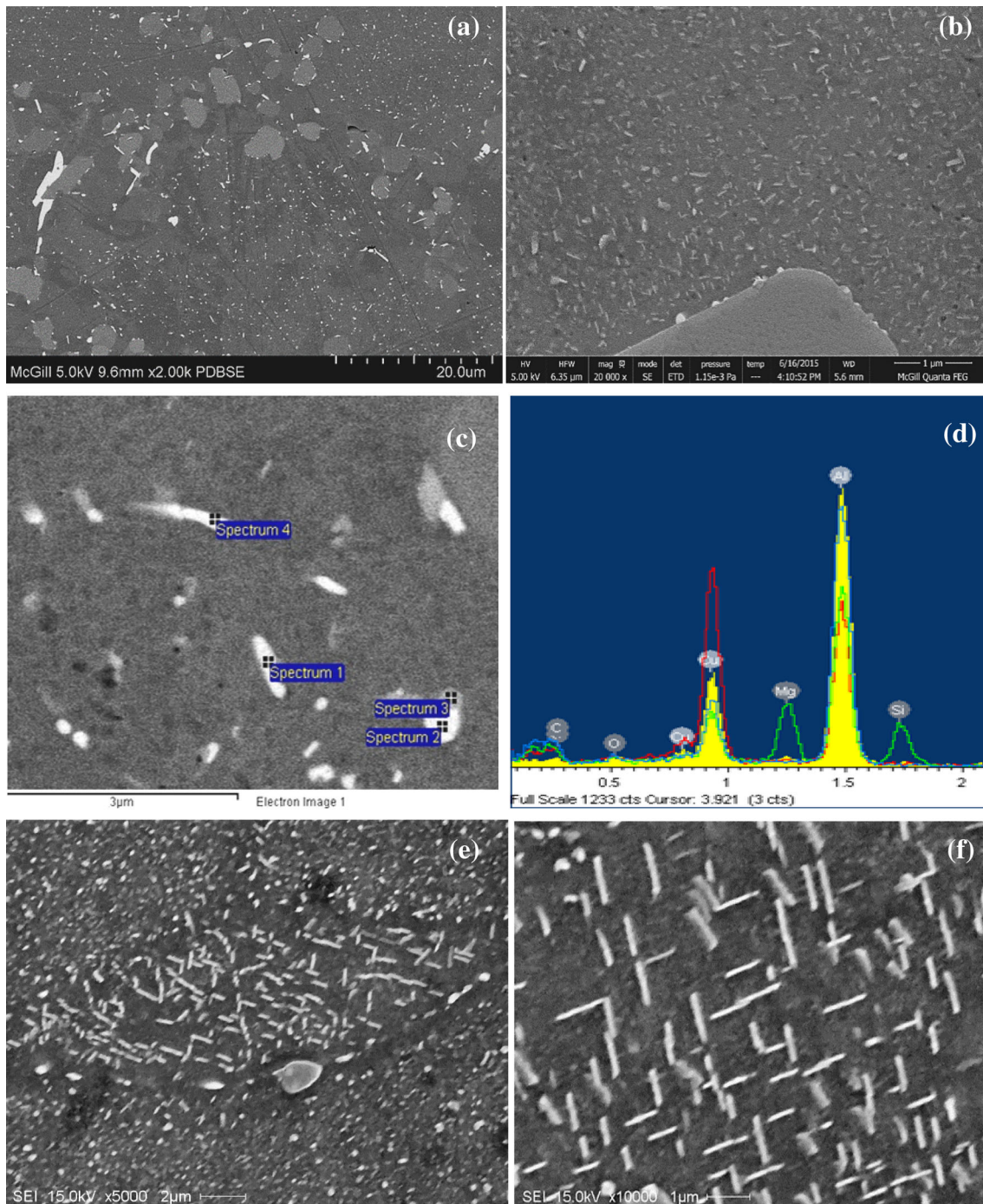
Figure 16. *(a) Backscattered image showing general view of the tensile sample of G5 alloy held at 300 °C/100 h prior to deformation, (b) no precipitate-free zones (PFZ) around the preexisting phases, (c) secondary electron image, (d) EDS spectra corresponding to (c), (e, f) high-magnification images of (a).*

354 alloys. Precipitates of $Al_3(Zr,Ti)$ with an ordered $L1_2$ structure are also observed.

2. Limiting the solutionizing temperature to 505 °C or less minimizes the possibility of incipient melting of the ternary eutectic structure α-(Al)–Si–Al_2Cu. Limiting the solutionizing temperature to 505 °C also helps to limit the growth of as-cast porosities.

3. During solutionizing process, the π-Fe phase decomposes into thin (100–300 nm) platelets of β-Fe which may reflect on the alloy performance.

4. The solution heat treatment temperature of 505 °C in combination with the aging temperature (190 °C/2 h) increases the alloy strength (UTS and YS) while maintaining more or less the

same ductility as that observed in the as-cast condition.

5. The influence of minor additions of Ni and Zr on the high-temperature performance of 354-type alloys is controlled by their T6-properties at room temperature, and by the temperature of testing and holding time prior to testing.

6. The addition of 0.4 wt% Ni + 0.4 wt% Zr is not sufficient to resist softening at 300 °C/100 h (observed after T6 treatment). However, T6 heat treatment of alloy containing 0.2 wt% Ni and 0.2 wt% Zr improves the tensile properties considerably, compared to the as-cast condition.

7. The addition of 0.4 wt% Ni leads to a decrease in the tensile properties, compared to the base alloy. This decrease may be attributed to a Ni–Cu reaction which could interfere with the formation of the Al_2Cu strengthening precipitates, thereby affecting the age-hardening process.

8. Holding the tensile samples of T6-treated base alloy resulted in a marked increase in the density of precipitated particles, most of the particles maintaining a spherical shape. Also, aging the solutionized alloy at 190 °C for 2 h resulted in the precipitation of Al_2Cu phase particles.

9. The formation of precipitate-free zones around the preexisting phases indicates that these precipitates are mainly Al_2Cu phase. Increasing the aging time and hence the density of the Al_2Cu results in the disappearance of the PFZs.

10. Increasing the stabilization time prior to deformation to 100 h resulted in changing the morphology of the Al_2Cu precipitates from spherical particles to thin platelets.

11. The presence of fine $L1_2$ ($Al_3(Zr,Ti)$)-type precipitates is the main feature observed in the microstructure of the tensile samples of alloys containing 0.2–0.4 wt% Zr additions.

12. The EDS spectra obtained from different locations in samples tested at 300 °C after 10 h holding indicated the presence of Q-$Al_5Mg_8Si_6Cu_2$ phase and Al_3Ni phase.

Acknowledgments

REFERENCES

1. A.M.A. Mohamed, F.H. Samuel, S.A. Alkahtani, Microstructure, tensile properties and fracture behavior of high temperature Al–Si–Mg–Cu cast alloys. Mater. Sci. Eng. A **577**, 64–72 (2013)

2. H.M. Kandil, None-combustible water-based quenchants in forging shops for automotive parts—latest development, in *The 1st International Automotive Heat Treating Conference*, (Puerto Vallarta, Mexico, 1998), pp. 106–109

3. S. Seifeddine, The influence of iron and Mg content on the microstructure and tensile properties of cast Al–Si–Mg alloys, in *Vilmer Project-5.2 Casting*, (The School of Engineering Component Technology, Sweden, 2007)

4. G.H. Garza Elizondo, *Machinability of Al–(7–11%)Si Casting Alloys: Role of Free-Cutting Elements*, Master's Thesis, (Université du Québec à Chicoutimi, Chicoutimi, QC, 2010)

5. ASM Handbook, *Heat Treating of Aluminum Alloys*, vol. 4, 10th edn. (American Society for Metals, Materials Park, OH, 1991)

6. D.G. Eskin, Decomposition of supersaturated solid solutions in Al–Cu–Mg–Si alloys. J. Mater. Sci. **38**, 279–290 (2003)

7. S.K. Son, M. Takeda, M. Mitome, Y. Bando, T. Endo, Precipitation behaviour of an Al–Cu alloy during isothermal aging at low temperatures. Mater. Lett. **75**, 629–632 (2005)

8. S.P. Ringer, K. Hono, Microstructural evolution and age hardening in aluminum alloys: atom probe field-ion microscopy and transmission electron microscopy studies. Mater. Charact. **44**, 101–131 (2000)

9. C.R. Hutchinson, S.P. Ringer, Precipitation processes in Al–Cu–Mg alloys microalloyed with Si. Metall. Mater. Trans. A **31A**, 2721–2733 (2000)

10. S. Abis, M. Massazza, P. Mengucci, G. Tiontino, Early ageing mechanisms in a high-copper AlCuMg alloy. Scr. Mater. **45**, 685–691 (2001)

11. G.E. Totten, D.S. Mackenzie, *Handbook of Aluminum: Physical Metallurgy and Processes*, vol. 1 (Marcel Dekker, NY, 2003)

12. S.C. Wang, M.J. Starink, N. Gao, Precipitation hardening in Al–Cu–Mg alloys revisited. Scr. Mater. **54**, 287–291 (2006)

13. P. Ratchev, B. Verlinden, P. De Smet, P. Van Houtte, Effect of cooling rate and predeformation on the precipitation hardening of an Al–4.2 wt%Mg–0.6 wt%Cu alloy. Scr. Mater. **38**(8), 1195–1201 (1998)

14. A. Charai, T. Walther, C. Alfonso, A.M. Zahra, C.Y. Zabra, Coexistence of clusters, GPB zones, S″-, S′- and S-phases in an Al-0.9 %Cu-1.7 %Mg alloy. Acta Mater. **48**, 2751–2764 (2000)

15. P. Ratchev, B. Verlinden, P. De Smet, P. Van Houtte, Precipitation hardening of an Al–4.2 wt%Mg–0.6 wt%Cu alloy. Acta Mater. **46**(10), 3523–3533 (1998)

16. C. Cayron, P.A. Buffat, Transmission electron microscopy study of the β′ phase (Al–Mg–Si alloys): ordering mechanism and crystallographic structure. Acta Mater. **48**, 2639–2653 (2000)

17. K. Matsuda, D. Teguri, T. Sato, S. Ikeno, EFTEM observation of Q' phase in Al–Mg–Si–Cu alloy. Mater. Sci. Forum **396–402**, 947–952 (2002)

18. J.Y. Hwang, R. Banerjee, H.W. Doty, M.J. Kaufman, The effect of Mg on the structure and properties of type 319 aluminum casting alloys. Acta Mater. **57**, 1308–1317 (2009)

19. G. Wang, Q. Sun, L. Feng, L. Hui, C. Jing, Influence of Cu content on aging behavior of AlSiMgCu cast alloys. Mater. Des. **28**, 1001–1005 (2007)

20. J. Buha, R.N. Lumley, A.G. Crosky, Microstructural development and mechanical properties of interrupted aged Al–Mg–Si–Cu alloy. Metall. Mater. Trans. A **37A**, 3119–3129 (2006)

21. G.A. Edwards, K. Stiller, G.L. Dunlop, M.J. Couper, The precipitation sequence in Al–Mg–Si alloys. Acta Mater. **46**, 3893–3904 (1998)

22. L. Ceschini, A. Jarfors, A. Morri, A. Morri, F. Rotundo, S. Seifeddine, S. Toschi, High temperature tensile behaviour of the A354 aluminum alloy. Mater. Sci. Forum **794–796**, 443–448 (2014)

23. J. Murray, A. Peruzzi, J.P. Abriata, The Al–Zr (aluminum–zirconium) system. J. Phase Equilib. **13**, 276–291 (1992)

24. D. Emadi, L.V. Whiting, M. Sahoo, J.H. Sokolowski, P. Burke, M. Hart, Optimal heat treatment of A356.2 alloy, in *Light Metals*, (The Minerals, Metals, and Materials Society, Warrendale, PA, 2003), pp. 983–989

25. D. Apelian, S. Shivkumar, G. Sigworth, Fundamental aspects of heat treatment of cast Al–Si–Mg alloys. AFS Trans. **97**, 727–742 (1989)

26. E.A. Elsharkawi, *Effects of Metallurgical Parameters on the Decomposition of π-AlFeMgSi Phase in Al–Si–Mg Alloys and Its Influence on the Mechanical Properties*, Ph.D. Thesis, (Université du Québec à Chicoutimi, Chicoutimi, QC, 2011)

27. M. Easton, W.Q. Song, T. Abbott, A comparison of the deformation of magnesium alloys with aluminum and steel in tension, bending and buckling. Mater. Des. **27**, 935–946 (2006)

28. Z. Li, A.M. Samuel, F.H. Samuel, C. Ravindran, S. Valtierra, H.W. Doty, Parameters controlling the performance of AA319-type alloys part I: tensile properties. Mater. Sci. Eng. A **A367**, 96–110 (2004)

29. E. Rincon, H.F. Lopez, M.M. Cisneros, H. Mancha, M.A. Cisneros, Effect of temperature on the tensile properties of an as-cast aluminum alloy A319. Mater. Sci. Eng. A **452–453**, 682–687 (2007)

30. D.H. St. John, L.M. Hogan, The peritectic transformation. Acta Metall. **25**, 77–81 (1977)

31. K.E. Knipling, *Development of a Nanoscale Precipitation-Strengthened Creep-Resistant Aluminum Alloy Containing Trialuminide Precipitates*, Ph.D. Thesis, (Northwestern University, Evanston, IL, 2006)

32. N.R. Andrade González, *Aging Effects in 319-Type Alloys*, Ph.D. Thesis, (McGill University, 2006)

33. F.J. Tavitas-Medrano, J.E. Gruzleski, F.H. Samuel, S. Valtierra, H.W. Doty, Effect of Mg and Sr-modification on the mechanical properties of 319-type aluminum cast alloys subjected to artificial aging. Mater. Sci. Eng. **480**(1–2), 356–364 (2008)

34. F.J. Tavitas-Medrano, A.M.A. Mohamed, J.E. Gruzleski, F.H. Samuel, H.W. Doty, Precipitation-hardening in cast Al–Si–Cu–Mg alloys. J. Mater. Sci. **45**, 641–651 (2010)

35. F.J. Tavitas-Medrano, S. Valtierra, J.E. Gruzleski, F.H. Samuel, H.W. Doty, 08-018 A TEM study of the aging behavior of 319 type alloys. AFS Trans. **116**, 99–114 (2008)

36. F.J. Tavitas-Medrano, J.E. Gruzleski, F.H. Samuel, S. Valtierra, H.W. Doty, Effect of Mg and Sr-modification on the mechanical properties of 319-type aluminum cast alloys subjected to artificial aging. Mater. Sci. Eng. A **480**, 356–364 (2008)

37. P. Prasad, *Characterization of New, Cast, High Temperature Aluminum Alloys for Diesel Engine Applications*, Master's Thesis, (University of Cincinati, Cincinati, 2006)

38. A.M. Nabawy, *Influence of Zirconium and Scandium on the Microstructure, Tensile Properties, and Hot-Tearing Susceptibility of Al–2 wt%Cu-Based Alloys*, Ph.D. Thesis, (Université du Québec à Chicoutimi, Chicoutimi, QC, 2010)

39. L. Bäckerud, G. Chai, J. Tamminen, *Solidification Characteristics of Aluminum Alloys, Foundry Alloys, Vol. 2*, (AFS/Skanaluminium, Des Plaines, IL, 1990)

40. S.G. Shabestari, S. Ghodrat, Assessment of modification and formation of intermetallic compounds in aluminum alloy using thermal analysis. Mater. Sci. Eng. A **467**, 150–158 (2007)